JOURNAL OF SOLID STATE CHEMISTRY **138,** 307–312 (1998)
ARTICLE NO. SC987789

A Structural Study of the Perovskite Series $Na_{1/2+x}La_{1/2-3x}Th_{2x}TiO_3$

Roger H. Mitchell and Anton R. Chakhmouradian

Department of Geology, Lakehead University, 955 Oliver Road, Thunder Bay, Ontario, Canada P7B 5E1

Received September 22, 1997; in revised form February 2, 1998; accepted February 17, 1998

An X-ray powder diffraction study of the series $Na_{1/2+x}La_{1/2-3x}Th_{2x}TiO_3$ is presented. The series comprises orthorhombic $CaTiO_3$-type perovskites (*Pnma*, $a \approx c \approx \sqrt{2}\,a_p$, $b \approx 2\,a_p$) in the range $0 \leq x \leq 0.083$ and tetragonal $La_{1/2}Li_{1/2}TiO_3$-type perovskites (*P4/mmm*, $a = a_p$, $c \approx 2a_p$) in the range $0.100 \leq x \leq 0.167$. The structure of the orthorhombic members is derived from the cubic aristotype by octahedral rotation. The degree of octahedral rotation is relatively small ($\Phi = 4.1$–7.6°), compared to that of other $CaTiO_3$-type perovskites. The tetragonal members of the series exhibit partial ordering of the cations at the *A*-site: the 1*a* and 1*b* sites are preferentially occupied by Na and Th, respectively. This results in alternate layers of Na and Th atoms perpendicular to the *c* axis of the tetragonal cell. Ti atoms are displaced from the center of the TiO_6 polyhedra due to the strong electrostatic repulsion effect of Th and La at the *A*-site. In contrast to previous studies, the end-member $Na_{2/3}Th_{1/3}TiO_3$ is shown not to have a cubic cell.

INTRODUCTION

The family of perovskite-type titanates includes a large number of compounds in which the *A*-site may accommodate alkali, alkaline-earth, rare-earth cations, Pb^{2+}, Fe^{2+}, Bi^{3+}, and Th^{4+}. Some complex perovskite-type titanates exhibit cation ordering at the *A*-site due to a large difference in radius between the *A*-site cations (1–3) or the presence of vacancies (4). An objective of the present work was to study structural characteristics of the series $Na_{1/2+x}La_{1/2-3x}Th_{2x}TiO_3$, which comprises perovskites with *A*-site cations significantly differing in both size and charge. This work was undertaken as part of a larger study of the crystallography of naturally occurring Th-bearing perovskite minerals and the sequestration of actinides in perovskite-type compounds for nuclear waste disposal. Due to the high tolerance of the perovskite structure toward cationic substitutions, perovskite-type titanates may be used as a major constituent of ceramic nuclear waste repositories (5–7).

The end-members of the solid solution series $Na_{1/2+x}La_{1/2-3x}Th_{2x}TiO_3$ have been synthesized by Belous *et al.* (8) and Zhu and Hor (9), respectively. A simple cubic perovskite structure (aristotype) was claimed for the $Na_{1/2}Ln_{1/2}TiO_3$ (Ln = La, Ce, Pr, Nd) perovskites (8, 10, 11). In contrast, Mitchell (12) suggested that $Na_{1/2}La_{1/2}TiO_3$ is orthorhombic (*Pnma*), and analogous to naturally occurring Na-*Ln* dominant perovskites (13). Based on the infrared spectra, Kaleveld *et al.* (14) have suggested that $Na_{1/2}La_{1/2}TiO_3$ displays partial ordering of the Na^{1+} and La^{3+} cations at the *A*-site. However, according to the X-ray diffraction studies of Kirsanov and Bazuev (10), the end-member $Na_{1/2}La_{1/2}TiO_3$ is not ordered; but in the series $Na_{3x}Ln_{2/3-x}TiO_3$, perovskites do undergo cation ordering with decreasing Na content (increasing number of vacancies). A double-cell cubic structure and partial ordering of Na^{1+} and Th^{4+} at the *A*-site were proposed for $Na_{2/3}Th_{1/3}TiO_3$ (9), although a rigorous assessment of the space group was not undertaken.

EXPERIMENTAL

Compositions corresponding to the series $Na_{1/2+x}La_{1/2-3x}Th_{2x}TiO_3$ were synthesized from stoichiometric amounts of Na_2CO_3, La_2O_3, ThO_2, and TiO_2 (high purity grade). The reagents dried at 150°C were mixed, ground in an agate mortar, and heated in air for 24 h initially at 1000°C to avoid the loss of Na. After regrinding, the samples were heated in air for 48 h at 1200°C and then rapidly cooled in air to the room temperature. X-ray diffraction (XRD) powder patterns of the synthesis products were obtained on a Philips 3710 diffractometer ($T = 20^\circ$C; radiation: Cu$K\alpha$; 2θ range 10°–145°; step $\Delta 2\theta$: 0.02°; time per step: 2 s). The XRD patterns were analyzed by the Rietveld method using the FULLPROF program (15). This program was chosen on the grounds that it provides an option to refine patterns composed of diffraction lines with differing line-width parameters (see below).

Composition of the samples was determined by X-ray energy-dispersion spectrometry (EDS) using a Hitachi 570 scanning electron microscope equipped with a LINK ISIS analytical system incorporating a Super ATW light element detector (133 eV FwHm Mn*K*). EDS spectra were aquired for 130 (live time) with an accelerating voltage of 20 kV and beam current of 0.86 nA. The spectra were collected and

0022-4596/98 $25.00

processed with the LINK ISIS-SEMQUANT software package. Well-characterized synthetic and naturally occurring standards were employed for the composition determinations: Th metal (Th), minerals loparite-(Ce) (Na, La), and perovskite (Ti). The accuracy of this method has been previously checked by wavelength-dispersion electron-microprobe analysis using an automated CAMECA SX-50 microprobe, following procedures described by Mitchell and Vladykin (16).

RESULTS AND DISCUSSION

A complete solubility was observed between the end-members of the series $Na_{1/2+x}La_{1/2-3x}Th_{2x}TiO_3$. The XRD patterns of both end-members and all intermediate members ($x \approx 0.0167n$, $n = 1$–9) show predominantly diffraction peaks of the perovskite-type phases. Minor diffraction lines indicative of ThO_2 are present on some XRD patterns, but their relative intensities do not exceed 1% of the strongest perovskite peak. The amount of vacancies at the *A*-site due to loss of Na is very small and comparable with the accuracy of EDS analysis (2 relative %).

In the compositional range $0 \leq x \leq 0.083$, the XRD patterns include several minor diffraction lines which cannot be indexed on a simple cubic cell (Table 1). The very low intensity of these lines and lack of obvious splitting of the strongest diffraction lines suggest that the deviation of the structure from aristotype is very small. Importantly, none of the XRD patterns in the compositional range $0 \leq x \leq 0.083$ shows superstructure peaks which may be indicative of the cation ordering. Therefore, in the Rietveld refinement, we used the structural model suggested by Mitchell (12): space group *Pnma*, $a \approx c \approx \sqrt{2}\,a_p$, $b \approx 2\,a_p$, $Z = 4$. In this model, the orthorhombic derivative of the perovskite structure is produced by $a^+b^-b^-$ or $a^+a^-a^-$ tilting (rotation) of octahedra about the three fourfold axes of the pseudocubic subcell (17, 18). For simplicity, the $a^+b^-b^-$ rotation may be interpreted as a combination of ϕ tilt about the *b* axis and θ tilt about the *c* axis in the orthorhombic lattice. This type of octahedral tilt can also be interpreted as one independent rotation Φ about one of the threefold axes of the pseudocubic subcell (19). The $a^+b^-b^-$ tilt is very common among perovskites and, at room temperature, occurs in $CaTiO_3$ and $NaMgF_3$ (17, 20).

Figure 1 illustrates a good agreement between the calculated and observed XRD patterns for $x = 0$. The crystallographic characteristics of two orthorhombic members of the $Na_{1/2+x}La_{1/2-3x}Th_{2x}TiO_3$ series ($x = 0$ and 0.05) are given in Table 2, and selected interatomic distances and bond angles for $x = 0$ in Table 3. The tilt angles ϕ, θ, and Φ were calculated from the unit-cell parameters using the equations given by Zhao *et al.* (20). Compared to other orthorhombic perovskites, the members of the $Na_{1/2+x}La_{1/2-3x}Th_{2x}TiO_3$ series exhibit relatively low tilt angles,

TABLE 1
X-Ray Diffraction Data for $Na_{1/2}La_{1/2}TiO_3$

h	*k*	*l*	*d* (Å)	I_{calc}	I_{obs}
1	0	1	3.873	2	2
0	2	0	3.871	1	1
2	0	0	2.745	24	26
1	2	1	2.742	100	100
0	0	2	2.740	22	22
1	1	2	2.337	1	1
2	2	0	2.239	13	16
0	2	2	2.236	11	13
2	0	2	1.939	38	42
0	4	0	1.938	20	21
1	4	1	1.734	1	1
1	0	3	1.733	1	1
3	2	1	1.584	18	19
2	4	0	1.582	9	9
1	2	3	1.582	20	20
0	4	2	1.582	8	8
4	0	0	1.372	5	5
2	4	2	1.371	20	21
0	0	4	1.370	4	5
3	2	3	1.226	8	8
2	0	4	1.225	3	3
1	6	1	1.225	7	7
4	2	2	1.170	2	2
2	6	0	1.169	1	1
2	2	4	1.169	1	1
0	6	2	1.169	1	1
4	4	0	1.120	5	5
0	4	4	1.120	4	4

e.g., for $x = 0$–0.083, Φ ranges from 4.1° to 7.6°, in contrast to $CaTiO_3$ and $NaMgF_3$, for which Φ is 10.3° and 17.8°, respectively (20, 21). In the $Na_{1/2+x}La_{1/2-3x}Th_{2x}TiO_3$ series, the rotation angles ϕ, θ, and Φ increase along with x and then rapidly decrease at $x = 0.083$, i.e., close to the transition point (Fig. 2).

Rietveld refinement of the XRD pattern for $x = 0$ using the DBWS program (22) also demonstrates a good agreement with the chosen model. The results of this refinement

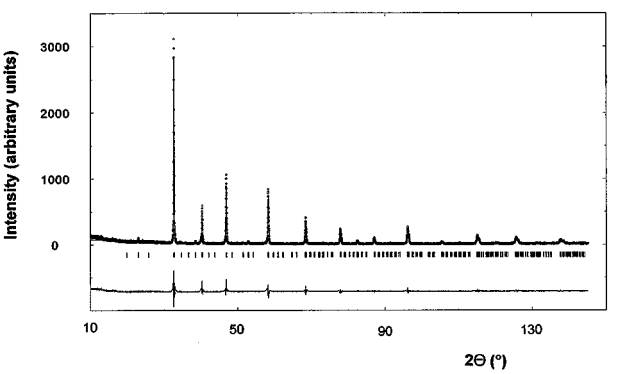

FIG. 1. Calculated (line) and observed (dots) XRD patterns and difference spectrum for $x = 0$.

TABLE 2
$Na_{1/2+x}La_{1/2-3x}Th_{2x}TiO_3$: Crystallographic Characteristics for $x = 0$ and 0.05 (in italic)

Atom	Position	x	y	z	B (Å^2)[a]
Na (La)	4*c*	− 0.0022(8)	1/4	0.0031(8)	0.63(3)
Na (La, Th)		*− 0.002(1)*		*− 0.001(1)*	*1.23(9)*
Ti	4*b*	0	0	1/2	0.50(3)
					1.04(7)
O1	4*c*	0.028(1)	1/4	0.548(1)	0.53(9)
		0.045(1)		*0.463(1)*	*2.3(2)*
O2	8*d*	0.241(1)	0.024(2)	0.258(2)	0.53(9)
		0.234(1)	*− 0.022(2)*	*0.263(2)*	*2.3(2)*

Note. Final agreement factors and cell parameters for $x = 0$: $R_p = 14.1$, $R_{wp} = 20.4$, $R_I = 5.0$, $\chi^2 = 1.38$, $a = 5.4736(4)$, $b = 7.7540(4)$, $c = 5.4785(4)$ Å; for $x = 0.05$: $R_p = 14.7$, $R_{wp} = 18.9$, $R_I = 6.7$, $\chi^2 = 1.85$, $a = 5.4542(5)$, $b = 7.7478(5)$, $c = 5.4704(4)$ Å.

[a] B factors are kept at the same values for all O atoms.

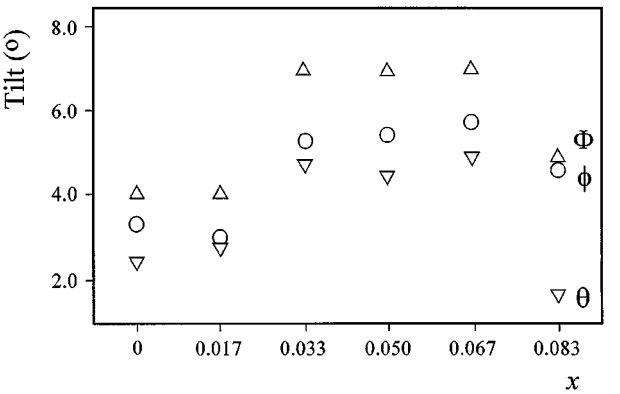

FIG. 2. $Na_{1/2+x}La_{1/2-3x}Th_{2x}TiO_3$ ($0 \le x \le 0.083$); variation of the tilt angles ϕ, θ, and Φ with the composition.

are comparable with those obtained in the present study. The unit-cell parameters and final agreement factors from the refinement using the DBWS program (Mitchell, unpublished data) are as follows: $R_p = 12.5$, $R_{wp} = 17.9$, $R_I = 4.9$, $\chi^2 = 1.35$, $a = 5.4743(4)$, $b = 7.7492(5)$, $c = 5.4802(3)$ Å.

In the compositional range $0.100 \le x \le 0.167$, the XRD patterns show the presence of broad superstructure lines due to ordering of the cations at the *A*-site (Table 4). A similar type of ordering at the *A*-site occurs between La^{3+} and Li^{1+} cations in $La_{2/3-x}Li_{3x}\square_{1/3-2x}TiO_3$ (2) and between La^{3+} and vacancies in $La_{2/3}TiO_{3-\lambda}$ ($0.007 \le \lambda \le 0.077$) (4). The superstructure lines decrease in intensity and become broader with decreasing x. As in the series $La_{2/3-x}Li_{3x}\square_{1/3-2x}TiO_3$ and $SrAl_{1/2}(Ta, Nb)_{1/2}O_3$, the broadening of the superstructure lines is undoubtedly related to the presence of antiphase domains (2, 23). Annealing of the end-member compound $Na_{2/3}Th_{1/3}TiO_3$ at 600°C for 10 days did not have any effect on the width or intensity of the superstructure lines. As noted above, Zhu and Hor (9) proposed for the end-member $Na_{2/3}Th_{1/3}TiO_3$ a double-cell cubic structure. However, the two possible models $Fm\bar{3}m$ and $Im\bar{3}$ in which $a \approx 2a_p$ may be eliminated because of reflection-limiting conditions. Also, it is noteworthy that the XRD patterns for $x = 0.100$–0.167 do not exhibit peak splitting typical of the ordered orthorhombic perovskites $La_{2/3}TiO_{3-\lambda}$ (4).

TABLE 3
$Na_{1/2+x}La_{1/2-3x}Th_{2x}TiO_3$: Selected Interatomic Distances (Å) and Angles (°) for $x = 0$

$x = 0$			
A–O1	2.501	O1–Ti–O1	180.0
A–O1	2.587	2 × O1–Ti–O2	76.7
A–O1	2.915	2 × O1–Ti–O2	82.7
A–O1	2.987	2 × O1–Ti–O2	97.3
2 × *d* *A*–O2	2.627	2 × O1–Ti–O2	103.3
2 × *d* *A*–O2	2.642	2 × O2–Ti–O2	89.5
2 × *d* *A*–O2	2.849	2 × O2–Ti–O2	180.0
2 × *d* *A*–O2	2.856	2 × O2–Ti–O2	90.5
2 × *d* Ti–O1	1.962	2 × O2–Ti–O2	180.0
2 × *d* Ti–O2	1.876	Ti–O1–Ti	162.3
2 × *d* Ti–O2	2.010	Ti–O2–Ti	170.2

Note: *A* = Na, La.

For the Rietveld refinement, we used a structural model assuming that "layers" populated predominantly by Na and Th, respectively, alternate along one of the fourfold axes of the cubic aristotype. The XRD patterns are best indexed in a primitive tetragonal cell (space group $P4/mmm$, $a = a_p$, $c \approx 2a_p$, $Z = 2$). Given the significant difference in width between the lines with $l = 2n$ and superstructure lines ($l = 2n + 1$), the patterns were refined using the two-phase option of the FULLPROF program following the procedure described by Fourquet *et al.* (2) with the "two" phases defined by the same structural model and differing only in line-width parameters. Calculated and observed XRD patterns for $x = 0.167$ are shown in Fig. 3, and crystallographic characteristics are given in Table 5. The cation occupancies at the 1*a* and 1*b* sites refined from the XRD patterns show that Th^{4+} is accommodated primarily at the 1*b*, while Na^{1+} at the 1*a* site (Table 5). With decreasing x (increasing La content), the difference between the cation occupancies at the two sites decreases, and the ratio $(1a)_{occ}/(1b)_{occ}$ approaches unity (Fig. 4). Both 1*a* and 1*b* sites are twelve-coordinated (4O1 + 8O2 for Na and 4O1 + 8O3 for Th), but the Th polyhedron is smaller than the Na polyhedron (Table 6), reflecting the difference in ionic radii of these elements: 1.21 Å and 1.39 Å, respectively (24). The Ti^{4+} cations are displaced from the centers of octahedra toward the O1 atoms; the estimated cation offset is approximately 0.15 Å. In the series $La_{2/3-x}Li_{3x}\square_{1/3-2x}TiO_3$, the Ti^{4+}

TABLE 4
X-Ray Diffraction Data for $Na_{2/3}Th_{1/3}TiO_3$

h	k	l	d (Å)	I_{calc}	I_{obs}
0	0	1	7.70	33	31[a]
0	0	2	3.847	2	2
1	0	0	3.845	3	3
1	0	1	3.444	26	31[a]
1	0	2	2.722	100	100
1	1	0	2.722	51	49
0	0	3	2.568	2	3[a]
1	1	1	2.566	5	6[a]
1	1	2	2.222	25	27
1	0	3	2.136	2	3[a]
0	0	4	1.926	17	16
2	0	0	1.924	37	35
1	1	3	1.868	10	11[a]
2	0	1	1.867	3	4[a]
1	0	4	1.722	2	2
2	0	2	1.722	2	1
2	1	0	1.721	1	1
2	1	1	1.679	6	8[a]
1	1	4	1.572	19	21
2	1	2	1.572	38	39
2	0	3	1.540	2	2[a]
1	0	5	1.431	4	4[a]
2	1	3	1.430	1	1[a]
2	0	4	1.361	18	16
2	2	0	1.361	10	9
2	2	1	1.340	1	2[a]
2	1	4	1.283	2	2
2	2	2	1.283	1	1
3	0	1	1.266	1	< 1[a]
1	0	6	1.218	7	7
3	0	2	1.217	8	7
3	1	0	1.217	8	7
3	2	3	1.202	1	2[a]
3	1	1	1.202	1	2[a]
1	1	6	1.161	2	2
3	1	2	1.160	3	3
2	1	5	1.148	4	4[a]
2	2	4	1.111	8	8
3	1	3	1.100	3	3[a]

[a] Broad line.

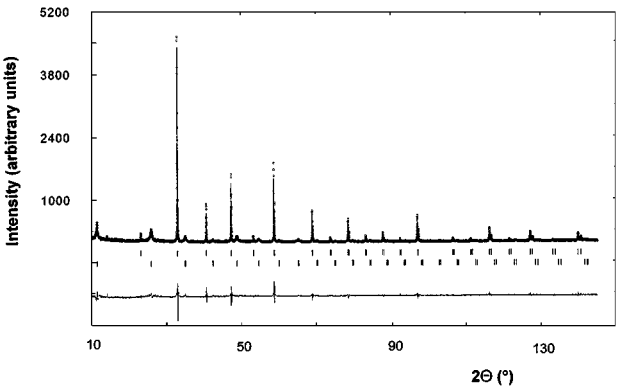

FIG. 3. Calculated (line) and observed (dots) XRD patterns and difference spectrum for $x = 0.167$.

cations are displaced toward the O2 atoms, i.e., in the opposite direction (2). The cation displacement in $La_{2/3-x}Li_{3x}\square_{1/3-2x}TiO_3$ ($x = 0.07$) estimated from data given by Fourquet *et al.* (2), is 0.14 Å. In both cases, the cation offset is toward the planes occupied by low-charge cations (Na^{1+} and Li^{1+}, respectively) and outward from the planes occupied by Th^{4+} and La^{3+}. This suggests that the cation displacement in the TiO_6 octahedra is driven by electrostatic repulsion effect between the high-charge *A*-site cations and Ti^{4+}.

In the series $Na_{1/2+x}La_{1/2-3x}Th_{2x}TiO_3$, the unit-cell dimensions gradually decrease with increasing x, i.e., increasing Th and decreasing La content (Table 7, Fig. 5). This compression of the structure reflects the much smaller ionic radius of Th^{4+} (1.21 Å), compared to La^{3+} (1.36 Å) (24). The structure undergoes transition from orthorhombic to tetragonal in the compositional range $0.083 \leq x \leq 0.100$. At $x = 0.083$, the a and c parameters of the orthorhombic cell are very close and, hence, the tilt angle θ is very small. Although the other component of octahedral rotation, angle Φ, remains relatively high and may be extrapolated into the tetragonal range ($0.100 \leq x \leq 0.167$), it does not have any physical meaning and would merely reflect the difference between the two unit-cell parameters. The transition involves partial ordering of the cations at the *A*-site due to the significant difference in radius between Na^{1+} and Th^{4+}. The refined cation occupancies suggest that La^{3+} favors the 1*b* site normally occupied by Th^{4+}. Although both Th^{4+} and La^{3+} cations are smaller than Na^{1+}, ionic radii of the latter two are quite similar, which could explain why the orthorhombic members of the series $Na_{1/2+x}La_{1/2-3x}$

TABLE 5
$Na_{1/2+x}La_{1/2-3x}Th_{2x}TiO_3$: Crystallographic Characteristics for $x = 0.167$

Atom	Position	Number of atoms	x	y	z	B (Å^2)[a]
Th1	1*a*	0.12	0	0	0	1.23(3)
Th2	1*b*	0.55	0	0	1/2	1.23(3)
Na1	1*a*	0.88	0	0	0	1.23(3)
Na2	1*b*	0.45	0	0	1/2	1.23(3)
Ti	2*h*	2	1/2	1/2	0.2335(8)	0.74(6)
O1	1*c*	1	1/2	1/2	0	3.7(2)
O2	1*d*	1	1/2	1/2	1/2	3.7(2)
O3	4*i*	4	0	1/2	0.275(1)	3.7(2)

Notes: Final agreement factors and cell parameters for the "two-phase" refinement: $R_p = 16.4$, $R_{wp} = 11.3$, $\chi^2 = 2.09$, $a = 3.8454(1)$, $c = 7.6965(3)$ Å. "Phase 1" ($l = 2n$): $R_I = 6.1$; "phase 2" ($l = 2n + 1$): $R_I = 19.4$.

[a] *B* factors are kept at the same values for all Th, Na, and O atoms.

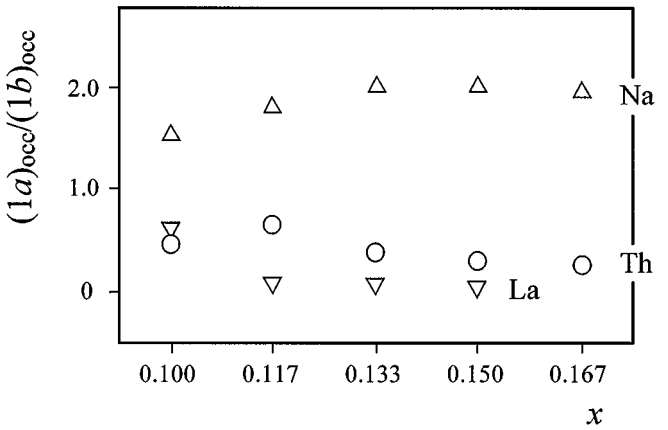

FIG. 4. $Na_{1/2+x}La_{1/2-3x}Th_{2x}TiO_3$ $(0.100 \leq x \leq 0.167)$; variation of the occupancy ratio $(1a)_{occ}/(1b)_{occ}$ with the composition.

TABLE 7
$Na_{1/2+x}La_{1/2-3x}Th_{2x}TiO_3$: Variation of Unit-Cell Parameters (Å)

x	a	b	c
		Orthorhombic	
0	5.4736(4)	7.7540(4)	5.4785(4)
0.017	5.4723(5)	7.7498(6)	5.4789(3)
0.033	5.4578(4)	7.7509(5)	5.4758(3)
0.050	5.4542(5)	7.7478(5)	5.4704(4)
0.067	5.4475(6)	7.7432(6)	5.4678(5)
0.083	5.4519(8)	7.7350(3)	5.4544(7)
		Tetragonal	
0.100	3.8564(4)		7.719(1)
0.117	3.8527(1)		7.7151(4)
0.133	3.8520(3)		7.701(1)
0.150	3.8494(1)		7.6963(6)
0.167	3.8454(1)		7.6965(3)

$Th_{2x}TiO_3$ show no ordering at the *A*-site. The absence of octahedral tilting in the structure of tetragonal members of the series cannot be explained unequivocally. In this study, we also tested two possible models involving both octahedral tilting and cation ordering at the *A*-site. These included P4/*nbm* ($a \approx \sqrt{2}\,a_p$, $c \approx 2\,a_p$, $Z = 4$) (Woodward, 1997, personal communication), and $P2_1/m$ ($a \approx b \approx \sqrt{2}\,a_p$, $c \approx 2\,a_p$, $\beta \neq 90°$, $Z = 4$). Both these models gave poorer fits with the experimental results, compared to the above-described *P*4/*mmm* model.

During this study, we also attempted to synthesize a K-analogue of the $Na_{2/3}Th_{1/3}TiO_3$ perovskite using K_2CO_3, ThO_2, and TiO_2 as starting reagents. The ordinary ceramic technique following the procedure described above for the $Na_{1/2+x}La_{1/2-3x}Th_{2x}TiO_3$ series, and synthesis from the melt ($T = 1300°C$) were employed. The examination of the synthesis products using X-ray diffraction and EDS, indicates that $K_{2/3}Th_{1/3}TiO_3$ does not form under ambient pressures. Both ceramic and melt syntheses lead to the formation of cubic ThO_2 and monoclinic $K_2Ti_6O_{13}$ (jeppeite). The incompatibility of K and Th within the perovskite structure presumably results from a large difference in ionic radii between these two elements (24).

TABLE 6
Selected Interatomic Distances (Å) and Angles (°) for $Na_{1/2}Th_{1/3}TiO_3$ and $La_{2/3-x}Li_{3-x}TiO_3$ ($x = 0.07$)

$Na_{2/3}Th_{1/3}TiO_3$		$La_{2/3-x}Li_{3-x}TiO_3$ ($x = 0.07$)	
$4 \times d$Na–O1	2.719	$4 \times d$La–O1	2.738
$8 \times d$Na–O3	2.857	$8 \times d$La–O3	2.765
$4 \times d$Th–O2	2.719	$4 \times d$Li–O2	2.738
$8 \times d$Th–O3	2.590	$8 \times d$Li–O3	2.723
dTi–O1	1.797	dTi–O1	2.083
dTi–O2	2.051	dTi–O2	1.806
$4 \times d$Ti–O3	1.948	$4 \times d$Ti–O3	1.939
O1–Ti–O2	180.0	O1–Ti–O2	180.0
O3–Ti–O3	161.3	O3–Ti–O3	173.6

Note: Distances and angles for $La_{2/3-x}Li_{3-x}TiO_3$ calculated from data given by Fourquet *et al.* (2).

CONCLUSIONS

The present work confirms the existence of a complete solid solution series between $Na_{1/2}La_{1/2}TiO_3$ and $Na_{2/3}Th_{1/3}TiO_3$. Thus, the perovskite structure can accomodate up to 46.7 wt.% ThO_2, provided that the charge balance is maintained by monovalent cations. X-ray powder diffraction study shows that the members of the series $Na_{1/2+x}La_{1/2-3x}Th_{2x}TiO_3$ are orthorhombic (*Pnma*) in the compositional range $0 \leq x \leq 0.083$, and tetragonal (*P*4/*mmm*) in

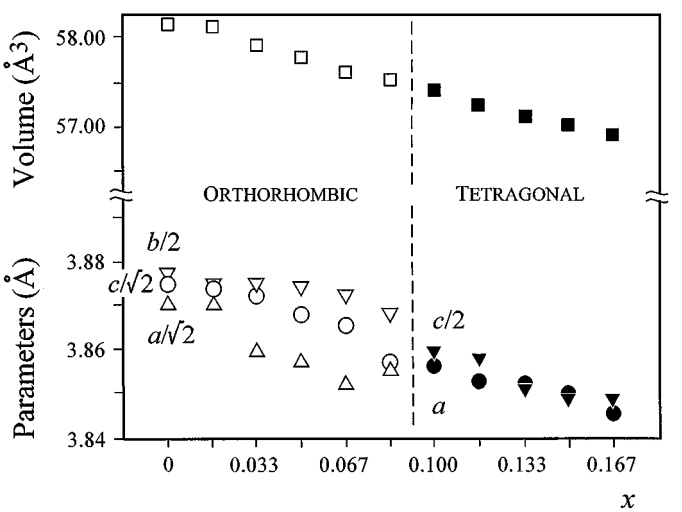

FIG. 5. $Na_{1/2+x}La_{1/2-3x}Th_{2x}TiO_3$; variation of the unit-cell parameters and volume (reduced to pseudocubic) with the composition.

the range $0.100 \leq x \leq 0.167$. The phase transition occurring between $x = 0.083$ and $x = 0.100$ involves partial ordering of Na, Th, and La at the *A*-site. In the most ordered structure ($x = 0.167$), 82% of the total amount of Th and 34% of the total amount of Na cations occupy the smaller 1*b* site. The "layers" comprising the 1*a* and 1*b* sites, respectively, alternate along the *c*-axis of the tetragonal cell. The orthorhombic members of the series show no cation ordering at the *A*-site, and stability of the perovskite-type structure is maintained through octahedral rotation. The data obtained in this study indicate that difference in ionic radii is a major factor controlling ordering at the *A*-site of the perovskite structure. HRTEM studies of $Na_{2/3}Th_{1/3}TiO_3$ are beyond the scope of this work, but are being undertaken in cooperation with J. L. Fourquet.

ACKNOWLEDGMENTS

This work was supported by the Natural Sciences and Engineering Research Council of Canada and Lakehead University, Ontario, Canada. We are grateful to Dr. J. L. Fourquet for the discussion on use of the FULLPROF program and Dr. J. Rodriguez-Carvajal for providing an access to this program. We also wish to thank Drs. Patrick M. Woodward, Andy MacDonald, and Gregory Lumpkin for numerous constructive comments on the early version of the manuscript.

REFERENCES

1. A. Varez, F. Garcia-Alvarado, E. Moran, and M. A. Alario-Franco, *J. Solid State Chem.* **118,** 78 (1995).
2. J. L. Fourquet, H. Duroy, and M. P. Crosnier-Lopez, *J. Solid State Chem.* **127,** 283 (1996).
3. K. Leinenweber, H. Linton, A. Navrotsky, Y. Fei, and J. B. Parise, *Phys. Chem. Miner.* **22,** 251 (1995).
4. M. Abe and K. Uchino, *Mater. Res. Bull.* **9,** 147 (1974).
5. A. E. Ringwood, S. E. Kesson, N. G. Ware, W. Hibberson, and A. Major, *Nature* **278,** 219 (1979).
6. A. B. Harker, *in* "Radioactive Waste Forms for the Future," p. 335. Amsterdam, North Holland, 1988.
7. G. R. Lumpkin, M. Collela, K. L. Smith, R. H. Mitchell, and A. O. Larsen, *in* "Scientific Basis for Nuclear Waste Management XXI." Mater. Res. Soc. Symp. Proceed, 1997 (in press).
8. A. G. Belous, G. N. Novitskaya, L. G. Gavrilova, S. V. Polyanetskaya, and Z. Ya. Makarova, *Soviet Progress Chem.* **51,** 13 (1985).
9. W. J. Zhu and P. H. Hor, *J. Solid State Chem.* **120,** 208 (1995).
10. N. A. Kirsanov and G. V. Bazuev, *Zh. Neorg. Khim.* **33,** 2909 (1988).
11. N. A. Kirsanov, G. V. Bazuev, and L. D. Finkel'shtein, *Zh. Neorg. Khim.* **33,** 1004 (1988).
12. R. H. Mitchell, *in* "Rare Earth Minerals: Chemistry, Origin and Ore Deposits," p. 41. Chapman & Hall, London/New York, 1996.
13. M. Hu, H.-R. Wenk, and D. Sinitsyna, *Am. Mineral.* **77,** 359 (1992).
14. E. W. Kaleveld, D. J. Bruntinck, J. P. Dotman, and G. Blasse, *J. Inorg. Nucl. Chem.* **35,** 3930 (1973).
15. J. Rodriguez-Carvajal, "FULLPROF Program: Rietveld Pattern Matching Analysis of Powder Patterns." ILL, Grenoble, 1990.
16. R. H. Mitchell and N. V. Vladykin, *Mineral. Mag.* **57,** 651 (1993).
17. A. M. Glazer, *Acta Crystallogr. Sect. B* **28,** 3384 (1972).
18. P. M. Woodward, *Acta Crystallogr. Sect. B* **53,** 32 (1997).
19. M. O'Keeffe and B. G. Hyde, *Acta Crystallogr. Sect. B* **33,** 3802 (1977).
20. Yu. Zhao, D. J. Weidner, J. B. Parise, and D. E. Cox, *Phys. Earth Planet. Inter.* **76,** 1 (1993).
21. X. Liu and R. C. Liebermann, *Phys. Chem. Miner.* **20,** 171 (1993).
22. R. A. Young, A. Sakhtivel, T. S. Moss, and C. O. Paiva-Santos, *J. Appl. Crystallogr.* **28,** 366 (1995).
23. P. Woodward, R.-D. Hoffmann, and A. W. Sleight, *J. Mater. Res.* **9,** 2118 (1994).
24. R. D. Shannon, *Acta Crystallogr. Sect. A* **32,** 751 (1976).